Experimental study of photoionization of ozone in the 12 to 21 eV region

A. Mocellin, K. Wiesner, F. Burmeister, O. Björneholm, and A. Naves de Brito

Citation: The Journal of Chemical Physics **115**, 5041 (2001); doi: 10.1063/1.1394945

View online: http://dx.doi.org/10.1063/1.1394945

View Table of Contents: http://scitation.aip.org/content/aip/journal/jcp/115/11?ver=pdfcov

Published by the AIP Publishing

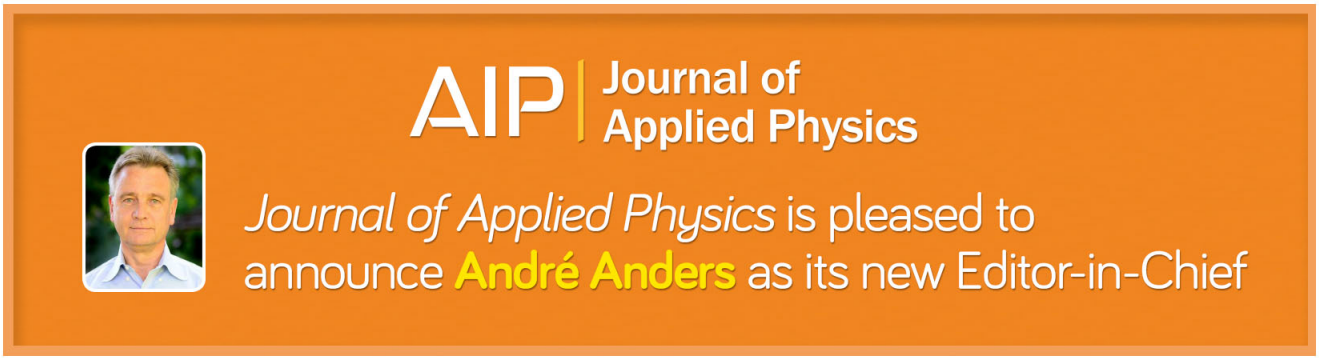

Experimental study of photoionization of ozone in the 12 to 21 eV region

A. Mocellin
Laboratório Nacional de Luz Síncrotron (LNLS), Box 6192 CEP, 13084-971 Campinas SP, Brazil and Institut of Physics Gleb Wataghin, University of Campinas, Brazil

K. Wiesner, F. Burmeister, and O. Björneholm
Department of Physics, Uppsala University, Box 530, S-751 21 Uppsala, Sweden

A. Naves de Brito[a)]
Laboratório Nacional de Luz Síncrotron (LNLS), Box 6192 CEP, 13084-971 Campinas SP, Brazil and Institute of Physics, University of Brasilia, Brazil

(Received 20 April 2001; accepted 27 June 2001)

The total and partial ion yield of ozone using time-of-flight is presented. The measurements were done using multicoincidence between a photoelectron and a photoion (PEPICO). Comparison with the photoelectron spectrum and previous measurements using other techniques allowed the assignment of most broad features in the spectra. Kinetic energy released is obtained for O^+ and O_2^+ ions. A discussion about the dissociation channels is included. © *2001 American Institute of Physics.* [DOI: 10.1063/1.1394945]

I. INTRODUCTION

During the last decades, ozone has attracted considerable attention from the general public after it has been pointed out that it presents an absorption band around 4.5 eV. In the stratosphere the presence of the ozone layer blocks biologically harmful UV radiation, due to this band, from reaching earth's surface. Otherwise, the presence of this radiation, strongly absorbed by human tissues, may cause cancer and other diseases. A number of studies present in the literature are concerned about the absorption spectrum below the first ionization threshold at 12.52 eV. The first study showing absorption spectrum above the ionization threshold comes from Ogawa and Cook.[1] However, few studies can be found above this limit.[2–4] An understanding of the ozone photochemistry above the ionization limit shall give key information on understanding the formation and destruction of ozone in higher atmosphere. In fact, ionic species are known to be extremely reactive and even a small number of these species may play an important role in ozone production and destruction in the stratosphere.

More studies can be found in the literature related to the photoelectron spectra where the different ionic states are assigned.[5–8] In our present studies the assignments from the photoelectron spectrum (PES) states will be used in the understanding of the ion yield spectrum above the ionization threshold. Very recently, both PES and resonant Auger spectra were recorded using synchrotron radiation as excitation source.[9] Valence ionic states can be resonantly populated even outside the ground state's Franck–Condon region. These other unknown states can be important to explain predissociation of the states reached through direct photoionization. See for example studies on O_2.[10]

The absorption above ionization threshold is closely related to the total ion yield spectrum where for each photon absorbed an ion is produced. Different dissociation channels may produce different composition of an ion and neutral fragments. Therefore, following each partial ion yield, important information about each dissociation channel for a certain state can be obtained. In this work, we present the partial ion yield of ozone between 12 and 21 eV. The assignments of these spectra are also discussed.

II. EXPERIMENT

Synchrotron radiation from the Brazilian Synchrotron Light Source (LNLS)[11] was used. The excitation beam was monochromatized by a toroidal grating monochromator (TGM) beamline that provides linearly polarized bending magnet radiation. The usable photon energy range in this beamline is from 12 to 300 eV.[12] The photon energy resolution, from 12 to 30 eV, is given by $E/\Delta E = 550$. This allows experiments with vibrational resolution to be performed.

The ions produced by photoionization and photodissociation were detected using a time-of-flight (TOF) mass spectrometer of Wiley–MacLaren type, constructed at the Institute of Physics, Brasilia University, Brasilia, Brazil.[13]

The axis of the TOF spectrometer is perpendicular to the photon beam and in the plane of the storage ring. A strong electric field is applied in the ionization region to collect one electron in the detector positioned in front of TOF tube, creating a start signal. The ions produced are accelerated in the opposite direction. After traveling through the TOF drift tube they hit a multi-channel plate (MCP) detector. Each ion reaching the detector will send a stop signal. Differences in the arrival times for different ions give information about the ions mass-to-charge ratio, and the form of the peaks gives information about the kinetic energy release and comparative abundance of each ion during the photon reaction.

The ozone gas was produced by electric discharging pure O_2 using a commercial ozonizer. In this process, a mixture of 10% ozone and 90% oxygen is obtained. An ozone concentration larger than 80% was obtained by a purification

a)Author to whom correspondence should be addressed. Electronic mail: arnaldo@lnls.br

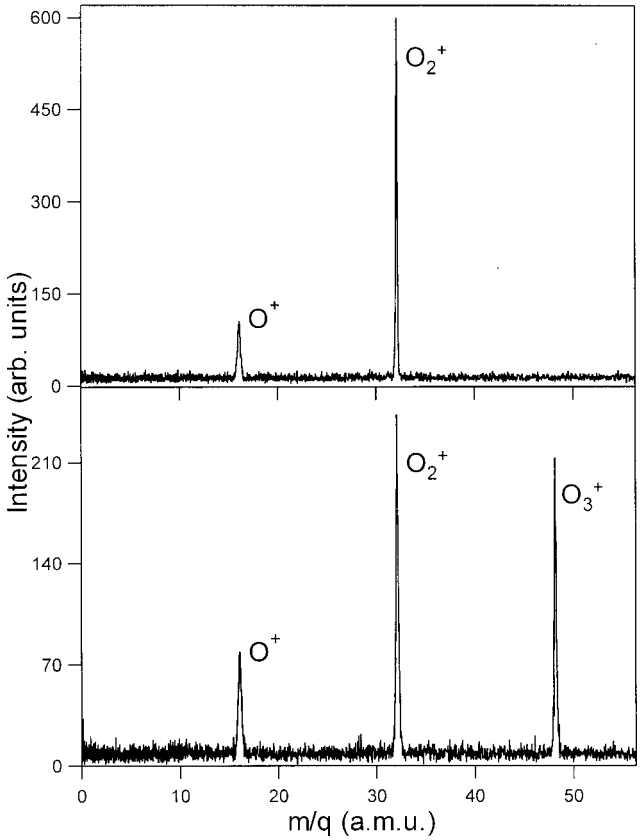

FIG. 1. PEPICO spectra of oxygen (top) and ozone bottom at 15.09 eV photon energy.

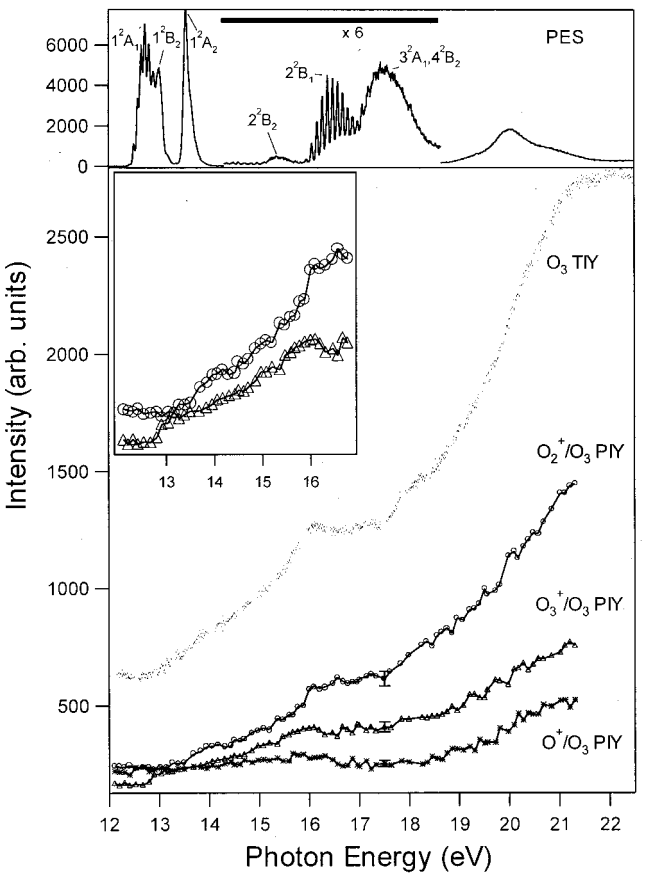

FIG. 2. Total (dots) and O_3^+, O_2^+, and O^+ (indicated in the figure) partial ion yield spectra of ozone. On top, PES of ozone from Ref. 9, in the region 14.4 to 18.6 eV, the spectrum is multiplied by 6. The inset in the graph shows the blow up of O_3^+ and O_2^+ partial ion yields of ozone, in the energy window from 12 to 16.5 eV.

process described in Ref. 14. Ozone should be carefully treated because it is very reactive and may explode during the purification process.

III. DATA ANALYSIS

In the present experiment, apart from the ozone total ion yield spectrum, we present, for the first time, the partial ion yield spectra using the photoelectron photoion coincidence technique (PEPICO). Information about the kinetic energy released after dissociation will also be given in the photon energy range studied.

Possible contributions from second- and higher-order light from the monochromator was checked by following the intensity of the pair O^+/O^+, which can only be produced by second and higher orders. A small intensity of this pair was found. Below the ionization threshold, a constant background, slightly higher for O_2^+ and O^+, was present which can be due to scattered, unmonochromatized light, which is expected to add a constant background.

Figure 1 shows a typical PEPICO spectra of O_3 and O_2 at 15.09 eV excitation energy. From right to left the products observed were O_3^+, O_2^+, O^+ for ozone and O_2^+, O^+ for molecular oxygen. Because the photon energy is below the double ionization threshold, there are no contributions of double ionization of ozone and oxygen molecules. The relative areas of the peaks reflect the relative abundance of each ionic species and the width is proportional to the kinetic energy released (KER) during the photofragmentation process.

Due to the photodissociation $O_3+h\nu=O_2^++O+e$, which is likely to generate O_2^+ ions with KER large than zero, the O_2^+ from O_3 is broader than O_2^+ from molecular oxygen where no dissociation takes place. A thorough discussion of the KER distribution will be given below.

The total ion yield (TIY) spectrum together with the partial ion yields (PIYs) O_3^+, O_2^+, O^+ spectra of ozone are shown in Fig. 2 while the O_2^+, O^+ ion yields of oxygen are presented in Fig. 3. These spectra were normalized by the photon flux. Comparing these spectra of ozone and oxygen molecules we noticed a (less than 20%) contamination from molecular oxygen in the ozone gas. The effect of this contamination was removed by subtraction. The result of this procedure can be see in Fig. 4, where we show the TIY spectra of ozone before and after the contamination subtraction. Care was taken to make sure the amount of contamination remained constant during the whole run by measuring PEPICO spectrum at fixed photon energies before and after a series of runs. Within the error bars no change in the quantity of the contamination was observed. We adopted a conservative approach in the subtraction of the molecular oxygen;

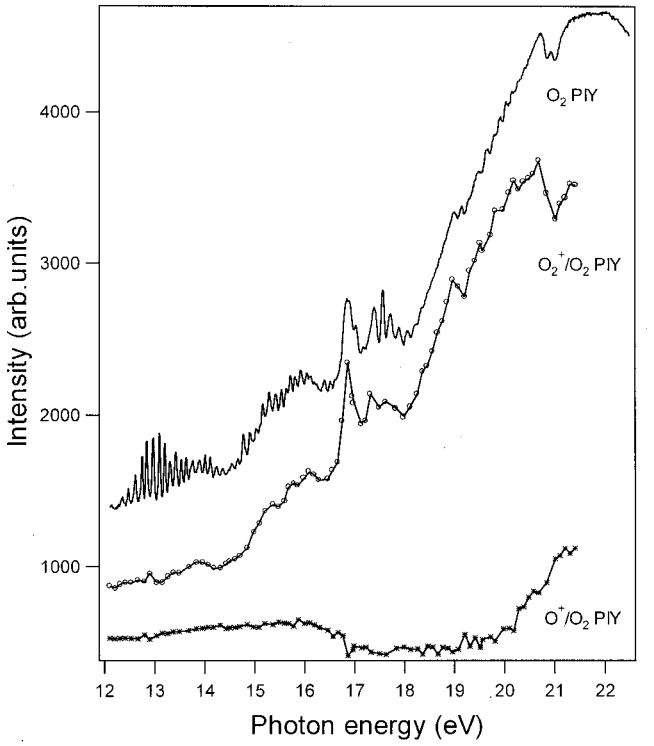

FIG. 3. Total (solid line) and O_2^+ and O^+ (indicate in the figure) partial ion yield spectra of oxygen.

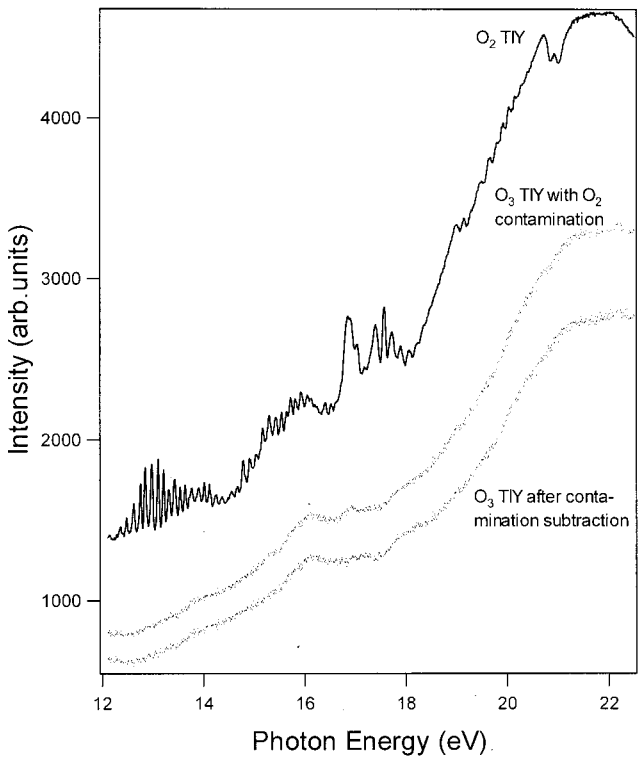

FIG. 4. Total ion yield spectra of molecular oxygen (solid line) and of ozone, with contamination (dots, in the middle) and after contamination subtraction (dots, in the bottom), in the region 12 to 22.5 eV.

therefore, the contamination may be slightly overestimated.

In order to maximize the ozone signal with respect to a small O_2 contamination, the photon energies used in the partial ion yield spectra were chosen not to coincide with the maximum of the molecular oxygen peaks. Therefore, in Fig. 3, both O_2^+ and O^+ partial ion yield spectra do not show the extensive vibrational bands present in the total ion yield.

One great advantage of using a TOF spectrometer is the possibility to compare the different dissociation channels (O_3^+, O_2^+, and O^+) directly. This is so because no ion is discriminated within a certain acquisition. Therefore, it is possible to determine the photoionization products at each energy and how they contribute to the TIY. The partial ion yield spectra are constructed from the time-of-flight spectra between 12 and 21 eV photon energy with steps of 0.1 eV except in a few energies where, for obvious reasons, a different step would improve the quality of the recorded data.

In the PIY spectra, each point corresponds to one time-of-flight spectrum measured at that photon energy. The intensity of each ionic fragment is obtained by fitting a Gaussian function to the time of flight spectra. The sum of these intensities is normalized by the corresponding intensity in the TIY spectrum.

The O_2 contamination was then removed from each O_3 PIY. The resulting spectra are shown in Fig. 2.

IV. RESULTS AND DISCUSSION

A. Discussion about the total ion yield

In both molecules, the total spectrum intensity increases with the photon energy. We can identify in the ozone spectrum, Fig. 2, an increase in the total ion yield around 12.5 eV which coincides with the ionization threshold. Using the simplest model available we can expect an increase in the ion production every time a new ionic state is reached. Indeed, when the first bound ionic state is reached, O_3^+ ions starts to be produced. The production of O_2^+ and O^+ ions may or may not coincide exactly with the ionization energy identified in the PES. If the ionic state has a dissociation channel leading directly to the production of the observed fragment ions, there will be a coincidence. In bound states, however, excitation to the lowest vibrational state within the Franck–Condon region will give rise to O_3^+ production initially. By increasing the photon energy one can reach higher vibrational states which could predissociate or dissociate, leading to O_2^+ and O^+ fragments instead of O_3^+. This change in fragmentation pattern will affect partial ion yield but not the TIY. Therefore, in the TIY, a larger or smaller step will be observed every time one reaches a new ionic state. The magnitude of the step will depend upon the cross section. From the photoelectron spectra (PES) we know the energy position of each ionic state as well as their assignment. From the presence of vibrational progressions in the PES it is also possible to determine which states are bound within the Franck–Condon region. Also, if a certain vibrational mode is excited predominantly, one can infer which products could be more or less likely. In order to facilitate our studies we have added the PES on top of Fig. 2, taken from Ref. 9. For most cases, the above assumption that the O_3 TIY spectrum features coincide with openings of new ionization channels is correct, but one must mention also the possibility of shape resonances and perhaps two-hole two-particle excitations.

These excitations could create structures in the TIY spectrum not related to the PES. Let us take O_2 as a guideline on how likely these excitations could occur in reality. In O_2, a broad shape resonance was identified at 21.7 eV.[10] A similar shape resonance could be present in ozone at about the same energy.

The first change in the slope at 12.5 eV agrees well with the ionization energy of state $1\,^2A_1(6a_1)$. In this region, slightly higher in energy, another overlapping state is present, $1\,^2B_2(4b_2)$.[5] A weak band is present around 14 eV, which can be assigned to the $1\,^2A_2(1a_2)$, with ionization energy equal to 13.5 eV. A large band between 15.4 and 17.5 eV is clearly observed. Within this band two peaks can be identified. The first peak with a maximum at 16.1 eV can be assigned to a mixture of two states, $2\,^2B_2$ and $2\,^2B_1$.[5] The second peak at 17.2 eV corresponds to the states $3\,^2A_1$ and $4\,^2B_2$. A weak feature is also present at around 18 eV, which is still in the region assigned to the states $3\,^2A_1$ and $4\,^2B_2$. It is interesting to notice that the last three states have a small ionization cross section in the PES spectrum and theoretical calculation could give important information about the assignment of the TIY spectrum. After this point the signal increases even more rapidly until 21.0 eV, and then the intensity stays almost constant up to 22.5 eV, the limit of our spectrum. This broad maximum around 21.5 eV, like in the O_2 molecule, could well come from shape resonance valence excitation.

B. Discussion about the partial ion yield

According to some later experiments, the adiabatic ionization potential (IP) of O_3^+ is around 12.52 eV[2] and for the other products even higher IPs are found. The small production of O_3^+, O_2^+, and O^+ below the IP is assigned to the presence of scattered light. This effect seems to give a larger production of O_2^+ and O^+ ions as compared to the O_3^+, which is probably caused by the presence of scattered light with shorter wavelength where the ion production would be dominated by the presence of dissociated species.

The O_3^+ PIY spectrum is presented in Fig. 2, showing an increasing intensity with the photon energy. The energy window from 12 to about 16 eV is blown up in the inset in the graph. We can identify a weak adiabatic production beginning at 12.7 eV, followed by an increasing in the intensity with a high slope. In this region, Weiss *et al.*[2] measured in the 12.519 to 12.924 eV window a series of seven steps using a magnetic mass spectrometer. The location of the onset for the steps can be correlated with the vibrational peaks observed in the first band of the ozone photoelectron spectrum, $1\,^2A_1$, assigned to the bending mode ν_2.[5] The second band, $1\,^2B_2$, in the photoelectron spectrum, between 13.00 and 13.34 eV, also presents a vibrational progression assigned to the symmetric stretch mode ν_1.[5] Our spectrum does not have enough resolution to determine the location of the steps, but it is clear that the two first bands of the photoelectron spectrum appear in this region in our O_3^+ PIY spectrum. We can confirm that the two states, $1\,^2A_1(6a_1)$ and $1\,^2B_2(4b_2)$, are bound and, after ionization, O_3^+ is produced.

Yet in the O_3^+ PIY spectrum we can see a large band between 15.4 and 16.5 eV with a maximum at 16.1 eV that coincides with the first maximum of the large band in TIY spectrum. We conclude that the O_3^+ makes a big contribution to this band in the TIY spectrum and it can be assigned to the $2\,^2B_2$. The intensity of O_3^+ rises rapidly after 18.9 eV.

In the partial ion yield O_2^+ spectrum from ozone the rise in the O_2^+ production occurs at 13.2 eV, leading to a small band with a maximum around 14.1 eV. This band coincides with the ionic $1\,^2A_2(1a_2)$ state (see the PES spectrum in Fig. 2). As we discussed before, the rise in the fragment ion production does not need to coincide with the ionization energy in the PES, although in this case it does. This will only be true for dissociative states or predissociative states with a crossing in the lowest Franck–Condon allowed vibrational state. This is probably true for the present case. If the crossing leading to predissociation takes place at higher vibrational energies, the position of the rise in the PIY will be shifted to higher energies by the same amount. According to theoretical calculations[15] the $1\,^2A_2$ state has an electron density mainly localized at the terminal oxygen atoms. For the lowest two states, $1\,^2A_1$ and $1\,^2B_2$, the situation is less clear and these orbitals may be delocalized. The rise in the O_2^+ PIY at 14.1 eV can hardly be seen in the O_3^+ PIY. Therefore, the dissociative or predissociative character of this state is anticipated. Indeed, according to Katsumata, this state may be predissociative and only a faint vibrational structure was assigned to the symmetrical vibrational stretching mode. The PIY also presents structures similar to the TIY spectrum between 15.6 and 17.5 eV. Three maxima can be found in this region, the first one at 16.1 and the second between 16.7 and 17.2 eV. They correspond to the states labeled, in the TIY spectrum, as, $2\,^2B_2$ (15.6 eV) and $2\,^2B_1$ (16.5 eV). In the PES the $2\,^2B_1$ state contains an extensive vibrational progression assigned to the symmetric stretching mode. At the O_3^+ PIY there is a decrease in the intensity, which can indicate a predissociative character for this state. The first peak at 16.1 eV can also be identified in the O_3^+ PIY indicating that the molecular ionic states are initially populated leading to the dissociation into $O_2^+ + O$. The states $3\,^2A_1$ and $4\,^2B_2$ (17.6 eV) do not present distinct vibrational progressions in the PES and thus can be dissociative. Possibly they can be related to the O_2^+ rise above 18 eV. The weak feature present at around 18 eV in TIY spectrum is well seen in O_2^+ PIY spectrum. The intensity of O_2^+ increases even more steeply than O_3^+ after 17.5 eV, giving more contribution than the other fragments to the TIY spectrum, in this energy region a valence shape resonance can be responsible for this broad feature.

The O^+ partial ion yield spectrum does not present clear structures. The most evident aspect in this spectrum is an increase in the signal after 18.3 eV. The discussion about this channel in ozone will profit from an analysis on the same channel in molecular oxygen, which has been studied in greater detail in the literature. If we compare our molecular oxygen O^+ partial ion yield spectrum with the analysis presented in Ref. 16, we notice that the O^+ production at about 18.7 eV coincides with the one observed in our spectrum. According to Ref. 16, this channel was assigned to the dis-

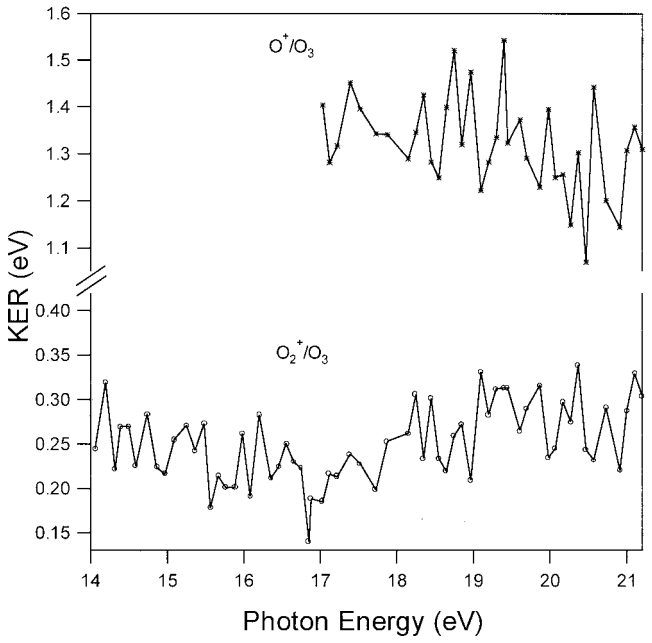

FIG. 5. Kinetic energy release of O^+ (top) and O_2^+ (bottom) fragments from ozone. The vertical axis is broken in two parts to better represent the results.

sociation of O_2^+ into $O^+ + O$. Another channel at lower energy was also assigned coming from the ion pair O^+/O^-. The presence of this channel is best identified if the apparatus can also detect negative ions, which we cannot do. In fact, it is difficult to identify this channel in our O^+ spectrum. The same situation may apply to ozone, i.e., an ion pair channel may exist for ozone, which we cannot easily identify with our apparatus. Measurements using a quadrupole mass analyzer would, in this case, be valuable. The increase in intensity in the O^+ channel at 18.3 eV is followed by a similar increase in the O_3^+ production. This seems to agree with the interpretation that an ionic state of O_3^+ is populated first, predissociating to the O^+ channel observed. This channel is lower in energy in ozone as compared to molecular oxygen.

Other information we were able to obtain was the O^+ and O_2^+ kinetic energy released (KER). Of course, the precision of the KER determination is limited in our case since we used a strong extraction field (70.8 V/mm) in order to avoid discrimination against ionic species. In the KER calculation we fitted fragment peaks using Gaussian functions. From the full width at half-maximum (FWHM) the full width at one-tenth of the maximum was obtained and used in the calculation. In it, the instrumental and thermal Doppler broadening were subtracted. The O_2^+ KER was 0.28 eV on average with small fluctuation through the whole window and O^+ KER was 1.3 eV, again small fluctuations were observed (see Fig. 5). In molecular O_2 the $O^+ + O$ pair is produced with low kinetic energy release (about 0.8 eV) in the two lower dissociation limits coming from predissociative states.[10] A larger kinetic energy release is expected for entirely dissociative states. We have compared our KER obtained for molecular oxygen with the one presented in Ref. 17. For the comparison we have chosen excitation energy of 21.05 eV. At this energy the signal to background ratio is very good. At lower photon energy our measurements for O_2 were always done at the valley of the O_2 resonant peaks. These measurements followed the O_3, in which we try to avoid the O_2 contamination. At 21.05 eV we obtained O^+ KER=1.1 eV, which compares well with the one given in Ref. 17. In that reference, the KER distribution peaked at 1.0 eV. In Fig. 5 we present the KER for both O_2^+ and O^+. We were careful to give the results in the range where good signal to background was present, thus avoiding excessive contamination of them from the small higher-order light contribution. These spurious contributions would tend to exaggerate the true KER.

V. CONCLUSIONS

The TIY was found to be composed of broad features although our resolution was certainly good enough to resolve several vibrational progressions in molecular oxygen. Using the ability of TOF spectroscopy to collect in parallel, without discrimination, ions produced through photoionization, we could directly compare the abundance of each ion. O_2^+ is certainly the most abundant species. This behavior is stronger at higher photon ionization in the interval studied. Comparison with the PES allowed the assignment of several broad structures observed in the PIY. Two states, $1\,^2A_2$ (dissociative) and $2\,^2B_1$ (predissociative with symmetric stretching vibration), were identified. These states presented peaks at the O_2^+ not present in the O_3^+ PIY spectrum. The KER for O^+ is far larger than that for O_2^+.

ACKNOWLEDGMENTS

The authors gratefully acknowledge the enthusiastic help of the LNLS staff. This research project has been supported by the National Council for Scientific and Technological Development (CNPq-Brazil), ''Fundação de Amparo a Pesquisa do Distrito Federal (FAP-DF Brazil),'' and Swedish Foundation for International Cooperation in Research and Higher Education (STINT).

[1] M. Ogawa and G. R. Cook, J. Chem. Phys. **28**, 173 (1958).
[2] M. J. Weiss, J. Berkowitz, and E. H. Appelman, J. Chem. Phys. **66**, 2049 (1977).
[3] R. J. Celotta, S. R. Mielczarek, and C. E. Kuyatt, Chem. Phys. Lett. **24**, 428 (1974).
[4] T. Gejo, K. Okada, and T. Ibuki, Chem. Phys. Lett. **277**, 497 (1997).
[5] S. Katsumata, H. Shiromaru, and T. Kimura, Bull. Chem. Soc. Jpn. **57**, 1784 (1984).
[6] C. R. Brundle, Chem. Phys. Lett. **26**, 25 (1974).
[7] J. M. Dyke, L. Golov, N. Jonathan, A. Morris, and M. Okuda, J. Chem. Soc., Faraday Trans. 2 **70**, 1828 (1974).
[8] N. J. Mason, J. M. Gingell, J. A. Davies, H. Zhao, I. C. Walker, and M. R. F. Siggel, J. Phys. B **29**, 3075 (1996).
[9] K. Wiesner, L. Rosenqvist, A. Naves de Brito *et al.* (unpublished).
[10] Y. Lu, Z. X. He, J. N. Cutler, S. H. Southworth, W. C. Stolte, and J. A. R. Samson, J. Electron Spectrosc. Relat. Phenom. **94**, 135 (1998).
[11] A. C. Lira, A. R. D. Rodrigues, A. Rosa *et al.*, Proc. EPAC, Stockholm (1998), and references therein.
[12] P. T. Fonseca, J. G. Pacheco, E. Samogin, and A. R. B. de Castro, Rev. Sci. Instrum. **63**, 1256 (1992).
[13] A. Naves de Brito, R. Feifel, A. Mocellin, A. B. Machado, S. Sundin, I. Hjelte, S. L. Sorensen, and O. Björneholm, Chem. Phys. Lett. **309**, 377 (1999).

[14] A. Naves de Brito, S. Sundin, R. R. Marinho, I. Hjelte, G. Fraguas, T. Gejo, N. Kosugi, S. Sorensen, and O. Björneholm, Chem. Phys. Lett. **328**, 177 (2000).
[15] N. Kosugi, H. Kuroda, and S. Iwata, Chem. Phys. **58**, 267 (1981).
[16] L. E. Berg, P. Erman, E. Källne, S. Sorensen, and G. Sundström, Phys. Scr. **44**, 328 (1991).
[17] P. Erman, A. Karawajczyk, E. Rachlew-Källne, M. Stankiewicz, and K. Yoshiki Franzén, J. Phys. B **29**, 5785 (1996).